

See discussions, stats, and author profiles for this publication at: <https://www.researchgate.net/publication/51666010>

# Live-Cell-Permeant Thiophene Fluorophores and Cell-Mediated Formation of Fluorescent Fibrils

ARTICLE in JOURNAL OF THE AMERICAN CHEMICAL SOCIETY · SEPTEMBER 2011

Impact Factor: 12.11 · DOI: 10.1021/ja2065522 · Source: PubMed

---

CITATIONS

28

READS

49

## 7 AUTHORS, INCLUDING:



[Francesca Di Maria](#)  
Italian National Research Council  
21 PUBLICATIONS 182 CITATIONS

[SEE PROFILE](#)



[Ilenia Viola](#)  
Italian National Research Council  
30 PUBLICATIONS 373 CITATIONS

[SEE PROFILE](#)



[Eduardo Fabiano](#)  
Italian National Research Council  
73 PUBLICATIONS 1,186 CITATIONS

[SEE PROFILE](#)

## Live-Cell-Permeant Thiophene Fluorophores and Cell-Mediated Formation of Fluorescent Fibrils

Ilaria Palamà,<sup>†</sup> Francesca Di Maria,<sup>§</sup> Ilenia Viola,<sup>||</sup> Eduardo Fabiano,<sup>†</sup> Giuseppe Gigli,<sup>†,‡</sup> Cristian Bettini,<sup>⊥</sup> and Giovanna Barbarella<sup>\*,§,⊥</sup>

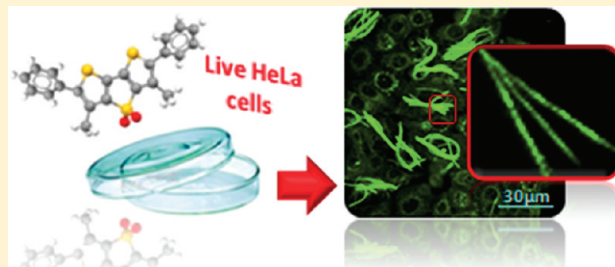
<sup>†</sup>NNL-CNR Nanoscience Institute and <sup>‡</sup>Dip. Ingegneria Innovazione, Università del Salento, Via Arnesano, 73100 Lecce, Italy

<sup>§</sup>Istituto for Organic Synthesis and Photoreactivity and <sup>⊥</sup>Mediteknology srl, National Research Council, Via Gobetti 101, 40129 Bologna, Italy

<sup>||</sup>NNL, Istituto Nanoscienze – CNR, via Arnesano, 73100 Lecce, and c/o Dipartimento di Fisica, Università La Sapienza, Rome, Italy

Supporting Information

**ABSTRACT:** In our search for thiophene fluorophores that can overcome the limits of currently available organic dyes in live-cell staining, we synthesized biocompatible dithienothiophene-S,S-dioxide derivatives (DTTOs) that were spontaneously taken up by live mouse embryonic fibroblasts and HeLa cells. Upon treatment with DTTOs, the cells secreted nanostructured fluorescent fibrils, while cell viability remained unaltered. Comparison with the behavior of other cell-permeant, newly synthesized thiophene fluorophores showed that the formation of fluorescent fibrils was peculiar to DTTO dyes. Laser scanning confocal microscopy of the fluorescent fibrils showed that most of them were characterized by helical supramolecular organization. Electrophoretic analysis and theoretical calculations suggested that the DTTOs were selectively recognized by the HyPro component of procollagen polypeptide chains and incorporated through the formation of multiple H-bondings.



### INTRODUCTION

In the past few years, interest in fluorescence optical imaging has grown exponentially in cell biology, biophysics, and biotechnology, prompted by advances in instrumentation<sup>1</sup> and light-emitting probes.<sup>2</sup> The increasing availability of sophisticated techniques and newly designed fluorescent probes opens new routes to cell exploration and expands the boundaries of possible discoveries and consequent industrial applications. On one hand, super-resolution methods—achieving nanoscale resolution in biological systems—offer unprecedented insights into specific cellular constituents and intracellular dynamics and processes.<sup>1</sup> On the other hand, more efficient synthetic methodologies allow the preparation of a wealth of new fluorophores: small organic molecules,<sup>3</sup> nanoparticles,<sup>4,5</sup> biocompatible<sup>6</sup> and nonblinking<sup>7</sup> quantum dots, polymer dots,<sup>8</sup> photoactivatable organic fluorophores,<sup>9</sup> target-cell-specific activatable probes,<sup>10</sup> and linear and branched conjugated oligo- and polyelectrolytes.<sup>11–13</sup> Meanwhile, genetically encodable fluorescent proteins evolve toward increasingly sophisticated applications for monitoring the inner components of live cells in real time.<sup>2</sup> All these dyes—acting with different modalities with living cells and their components and through different types of interactions—demonstrate the tremendous potential of fluorescence techniques for cell imaging and tracking, obtaining real-time mechanistic insights into protein aggregation processes and related diseases, and detection of modified optical and electronic properties at the cellular level.

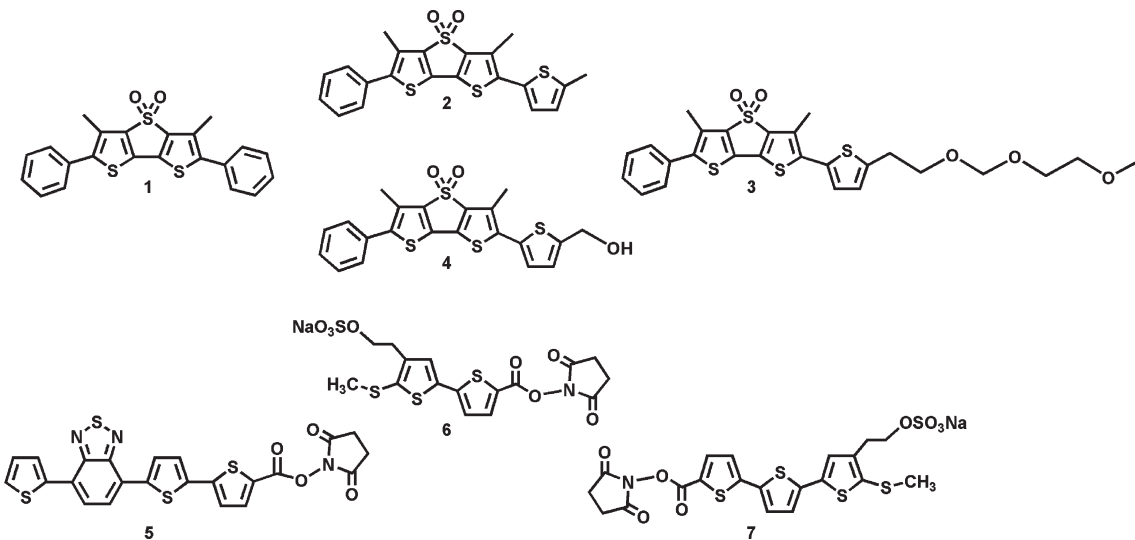
All fluorophores reported so far have limits and drawbacks. For example, fluorescent proteins cannot stain non-encodable cell components such as glycans, lipids, and DNA. Quantum dots, which have very appealing optical properties, are not genetically encodable, need mechanical methods such as micro-injection to get into the cells, and, once inside, are unable to target a specific protein. Moreover, they have to be coated with biologically compatible polymers and are scarcely reproducible.<sup>14</sup> Small fluorescent molecules, which are nano-objects of well-defined structure and dimension that can be engineered by organic synthesis, may also be difficult to load within the cells and retain for a sufficiently long time. Organic fluorophores with good retention times within the cells are scarce, as are those that uniformly and selectively stain the cytoplasmic compartments.<sup>15,16</sup> Furthermore, organic fluorophores often photobleach, becoming dark and consequently untraceable.

All types of fluorophores, to be useful, must be nontoxic to the cells, must have sufficiently high absorption coefficients and quantum yields, must have emission frequencies that are easy to discriminate from background autofluorescence, must not photobleach, and must have sufficiently large Stokes shifts to filter out the exciting light. Last, they should be low cost and easy to handle for extensive application with the instrumentation

Received: July 14, 2011

Published: September 27, 2011

Chart 1. Molecular Structure of the Fluorophores Described in This Study



commonly available in chemical, physical, and cell biology laboratories. All these requirements make the development of new fluorophores a rather complex task, since no precise criteria are available so far to predict their properties. Thus, researchers are more than ever involved in the search for better fluorophores that can overcome the limitations of those currently available.

In the past few years, we have developed a few families of thiophene fluorophores that are optically stable and have easily tunable properties.<sup>17</sup> While there are a fair amount of publications on thiophene oligomers and polymers as organic semiconductors,<sup>18</sup> the number of those describing their use as fluorescent markers for biological applications is very limited. Due to the versatile thiophene chemistry, the properties of thiophene fluorophores can be modulated to make them more robust, more brightly fluorescent, and easier to conjugate to molecules and polymers of biological interest.<sup>17</sup> However, so far, to be able to penetrate the membrane of living cells, they need to be conjugated to an appropriate carrier.<sup>19</sup> Consequently, the development of thiophene fluorophores with high living cell internalization efficiency remains challenging for application of these dyes to biological problems.

Here, we report a study describing novel biocompatible thiophene fluorophores capable of spontaneously penetrating the membrane of living cells and uniformly staining the cytoplasm with long-lasting fluorescence and no harm to the cells. In the course of this study, we discovered that some dithienothiophene-S,S-dioxide derivatives (DTTOs) are cell-permeant fluorescent dyes that cause the secretion of fluorescent fibrils by live cells. We describe the synthesis of the DTTOs, the formation of fluorescent fibrils when the DTTOs are administered to live cells, and the characterization of the fibrils by electrophoretic analysis, confocal microscopy, and atomic force microscopy (AFM). A hypothesis accounting for the formation of the fluorescent fibrils, based on experimental data and theoretical calculations, is reported and discussed.

## RESULTS AND DISCUSSION

**Synthesis.** The molecular structures of the fluorophores described in this study are shown in Chart 1.

The synthetic pattern for the preparation of compounds 1–4 is reported in Scheme 1, while the preparation of compounds 5–7 is reported in Schemes S2 and S3 in the Supporting Information. The synthesis of the fluorophores was carried out starting from commercial precursors and was based on Suzuki<sup>20</sup> and/or Stille coupling<sup>21</sup> in the presence of palladium catalysts. The fluorophores were prepared taking advantage of ultrasound (US) and microwave (MW) assistance. US and/or MW irradiation—low-energy, low-cost enabling technologies—allowed rapid and efficient preparations, the fluorophores being obtained in very pure form.

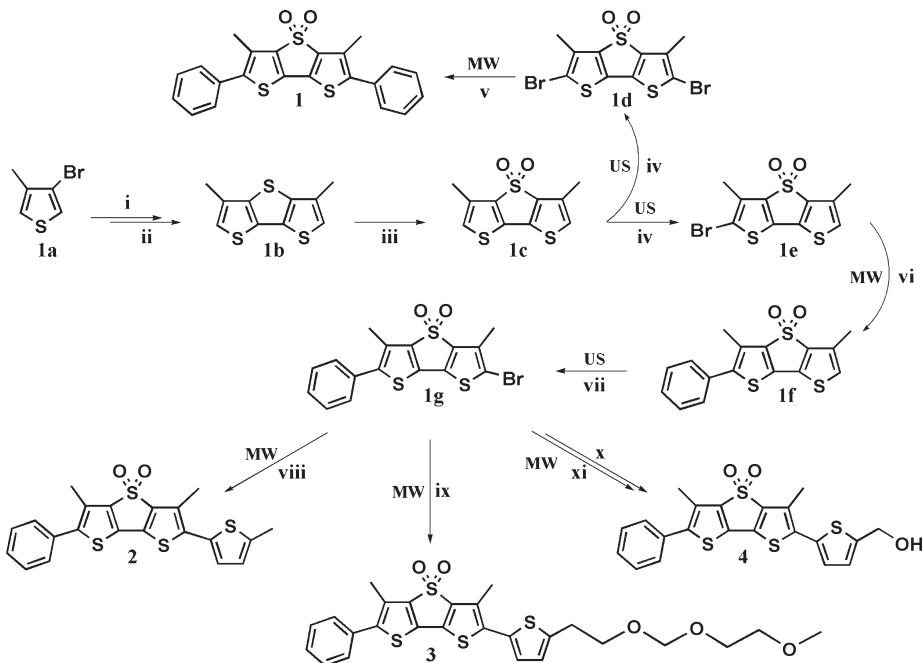
Compounds 1, 1b, 1c, and 1d had already been prepared through different synthetic pathways.<sup>22</sup> Here, the synthesis of the rigid 3,5-dimethyldithieno[2,3-d;3',2-b]thiophene inner core (1b) from 3-bromo-4-methylthiophene was made more expedient by employing commercial bis(*tri-n*-butyltin)sulfide to obtain the precursor bis(4-methylthiophen-3-yl) sulfide in 90% yield (see SI for details). Use of US irradiation allowed us to obtain the monobromo derivative 1e, almost free of the corresponding dibromo derivative (1d), in 80% yield in 30 min at room temperature, using NBS and CH<sub>2</sub>Cl<sub>2</sub>:CH<sub>3</sub>COOH (6:4 v/v) as the solvent. In the absence of US, NBS needed to be added stepwise during many hours, and the resulting product always contained a non-negligible amount of 1d. The reactions of the mono- and dibromo derivatives with the appropriate stannanes were carried out with MW assistance, which allowed us to obtain the desired compound rapidly (1 h) and in high yields (80–95%).

The detailed description of all compounds in Schemes 2, S1, and S2 is reported in the Supporting Information and in Figures S1–S26.

**Optical Properties.** Absorption and photoluminescence maximum wavelengths ( $\lambda_{\text{max}}$ ,  $\lambda_{\text{PL}}$ ), molar absorption coefficients ( $\epsilon$ ), and quantum yields ( $\phi$ ) of fluorophores 1–7 in DMSO are given in Table 1. The absorption and photoluminescence spectra are reported in Figure S27, together with the experimental details.

Table 1 shows that DTTOs 1–4 display the highest  $\phi$  values in DMSO, in the range 0.5–0.9, whereas the nonfused fluorophores 5–7 display values in the range 0.3–0.4, as expected for ter- and quaterthiophene in solution.<sup>22,23</sup> For 1, an absolute fluorescence quantum yield of 0.87 in dichloromethane, measured using an integrated sphere, has already been reported by us.<sup>22</sup>

**Scheme 1.** Ultrasound and Microwave-Assisted Synthesis of DTTO Fluorophores **1–4** from Commercial 3-Bromo-4-methylthiophene<sup>a</sup>



<sup>a</sup> Reagents and conditions: (i) bis(tri-*n*-butyltin) sulfide, Pd(PPh<sub>3</sub>)<sub>4</sub>, toluene, 130 °C, 90%; (ii) *n*-BuLi, CuCl<sub>2</sub>, ethyl ether, 0 °C, 50%; (iii) 3-chloroperbenzoic acid, CH<sub>2</sub>Cl<sub>2</sub>, 70%; (iv) 1 or 2 mmol of NBS, CH<sub>3</sub>COOH/CH<sub>2</sub>Cl<sub>2</sub>, US, 80%, 99%; (v) tributyl(phenyl)stannane, 5% Pd(PPh<sub>3</sub>)<sub>4</sub>, toluene, MW, 80 °C, 95%; (vi) tributyl(phenyl)stannane, 5% Pd(PPh<sub>3</sub>)<sub>4</sub>, toluene, MW, 80 °C, 95%; (vii) NBS, CH<sub>3</sub>COOH/CH<sub>2</sub>Cl<sub>2</sub>, US 30 min, room temperature, 99%; (viii), (ix), (x) tributyl(5-methylthiophen-2-yl)stannane, tributyl(5-(2-((2-methoxyethoxy)methoxy)ethyl)thiophen-2-yl)stannane, tert-butyldimethyl((5(tributylstannyl)thiophen-2-yl)methoxy)silane, 5% Pd(PPh<sub>3</sub>)<sub>4</sub>, toluene, MW, 1 h, 80 °C, 80%, 80%, 95%; (xi) Et<sub>3</sub>N·3HF, THF, 99%.

**Table 1.** Absorption ( $\lambda_{\text{max}}$ , nm) and Emission ( $\lambda_{\text{PL}}$ , nm) Wavelengths, Molar Absorption Coefficients ( $\epsilon$ ,  $\text{cm}^{-1} \text{M}^{-1}$ ), and Quantum Yields ( $\varphi$ ) of Fluorophores **1–7** in DMSO

compd	$\lambda_{\text{max}}$	$\lambda_{\text{PL}}$	$\epsilon$	$\varphi$	compd	$\lambda_{\text{max}}$	$\lambda_{\text{PL}}$	$\epsilon$	$\varphi$
1	408	514	18 030	0.85	5	479	613	26 142	0.34
2	430	544	22 393	0.49	6	346	428	12 645	0.30
3	429	543	22 397	0.50	7	409	589	20 873	0.42
4	428	542	20 079	0.51					

The  $\varphi$  values of Table 1 are only indicative of a possible trend within the cellular environment. Indeed, it is known that the viscous cellular milieu affects the fluorescence in a way that is very difficult to predict.<sup>17</sup> Probably, two opposing factors are operating within the cells. On one side, the increase in viscosity leads to the rigidification of the molecular skeleton, causing the increase of  $\varphi$ ; on the other, molecular aggregation causes a drop of  $\varphi$  with respect to the value in DMSO. We notice that, in the case of DTTO **1**, the absolute  $\varphi$  value drops to 0.24 on going from solution to microcrystalline powder.<sup>22</sup> Anyway, what we observe experimentally is that—whatever their precise  $\varphi$  value in the cellular environment—the fluorophores remain intensely fluorescent within the cells once they have crossed the cellular membrane.

The molar absorption coefficients of Table 1 are in line with those already reported for thiophene fluorophores in solution, in the range 12 000–26 000  $\text{cm}^{-1} \text{M}^{-1}$ .<sup>17</sup> All fluorophores display large Stokes shifts from absorption to emission wavelengths, also in line with the trend of thiophene fluorophores.<sup>17</sup> Compounds

**1–7** were also stable under prolonged irradiation at the maximum absorption wavelength, and neither appreciable photo-bleaching nor blinking was observed after many hours of exposure to the irradiation source, as already reported for thiophene fluorophores.<sup>17</sup>

**Cell Staining and Fluorescent Fibrils Formation.** The fluorophores displayed a different degree of solubility in water: poor solubility for DTTO fluorophores **1–4**, good solubility for the two alkylsulfonate-substituted fluorophores **6** and **7**, and insolubility for the benzothiadiazole-based **5**. Nevertheless, all of them had the right hydrophilicity/hydrophobicity balance and the stereoelectronic requirements needed to spontaneously cross the cell membrane.

Live NIH 3T3 cells—mouse embryonic fibroblast cells of mesodermal origin whose function is to form the structural fibrils of connective tissues, including collagen—and HeLa cells—cervical cancer cells—were employed for the staining experiments. No special loading procedures were needed, since all fluorophores were spontaneously taken up by the cells without apparent leakage. The cells were first incubated for 1 h with the different fluorophores in buffered solution, and then they were extensively washed with culture medium to remove the unbound fluorophore (see SI for details). Through a trial-and-error procedure it was found that the optimum fluorophore concentration in buffered solution was 0.05 mg/mL. After complete replacement of the culture medium, the cells were continuously cultured for several days and monitored at fixed times.

All fluorophores were able to stain with bright fluorescence the cytoplasm of the cells, while the nucleus remained dark. In all

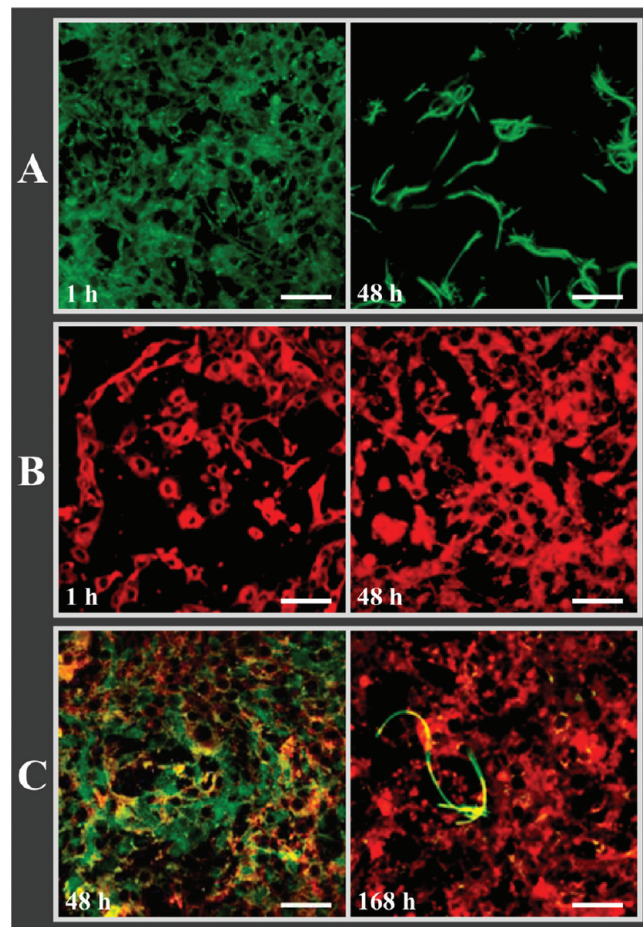


**Figure 1.** (A) Laser scanning confocal microscopy images of NIH 3T3 cells stained with fluorophores **1** taken 1 and 48 h after treatment and extensive washing. After 48 h, numerous fluorescent fibrils are present. (B) LSCM images of NIH 3T3 cells stained with thiophene-based *N*-hydroxysuccinimidyl ester **5** taken 1 and 48 h after treatment and washing. (C) Overlay of images of NIH 3T3 cells treated first with **5** and then with **1**, showing the formation of green fluorescent fibrils. Scale bars, 75  $\mu$ m.

cases, the fluorescence persisted for at least 7 days (the maximum time we were able to monitor the cells), during which the cells were normally proliferating, and was transmitted from mother to daughter cells during the replication process (Figures 1 and 2). However, there was a distinctive difference between the behaviors of fluorophores **5–7** and DTTO fluorophores **1–4** causing the production of fluorescent fibrils.

Fluorophores **5–7** stain the cytoplasm of live NIH 3T3 cells with bright and persistent fluorescence, as shown in Figure 1 for the red-emitting fluorophore **5**. Since these fluorophores are functionalized with the succinimidyl ester group (NHS), they are likely to be retained within the cells through the covalent binding of NHS to primary amino groups of intracellular proteins. It has been shown that this is indeed the mechanism leading to cytoplasm staining of live cells by carboxyfluorescein diacetate succinimidyl ester, one of the most commonly used dyes to stain the cytoplasm of living cells.<sup>24</sup> We have already demonstrated that, with thiophene *N*-succinimidyl esters, the reaction of NHS with primary amino groups of proteins to form an amidic bond is rapid and occurs at very low concentrations in mildly basic

conditions.<sup>17,25</sup> The same reaction cannot occur within the nucleus, the acidic region of the cell containing nucleic acids, which consequently is not stained.

Clearly, an alternative mechanism must operate with DTTO fluorophores **1–4** lacking the NHS functionality. Based on our observations, these fluorophores are first distributed uniformly into the cytoplasm; afterward they migrate to the perinuclear region of the cells and concentrate in multiple clusters, acting as nucleation areas for the formation of fibrils via a cell-mediated process. All this is illustrated in Figures 1 and 2.

Figure 1A compares the laser scanning confocal microscopy (LSCM) images of NIH 3T3 cells stained with fluorophore **1** with those of NIH 3T3 cells stained with *N*-hydroxysuccinimidyl ester **5**. In both cases the images were taken 1 and 48 h after treatment and extensive washing. It is seen that, after 1 h of treatment, the cytoplasmic regions are brightly green or red fluorescent, depending on the fluorophore, with no or undetectable staining of the nuclei. The bright red staining of the cells treated with **5** persisted after 48 h, during which the cells were normally proliferating (see below for the cytotoxicity tests) and the fluorescence was transmitted from mother to daughter cells. By contrast, in the cells treated with **1**, after 48 h there was the appearance of numerous fibrils, randomly oriented and so intensely fluorescent as to mask the emission of stained cells on the background. The amount of fluorescent fibrils formed increased progressively over time while the cells were normally proliferating (see below for the cytotoxicity tests). Their formation and progressive increase were reproducible and were verified several times with fresh cells and fresh fluorophore, always with the same results.

To confirm the different cell-labeling mechanisms of the two different types of fluorophores and simultaneously check whether the formation of fluorescent fibrils can take place also in the case of multilabeling of the cells, we treated NIH 3T3 cells with both fluorophore **5** and fluorophore **1**.

NIH 3T3 cells were first incubated for 1 h with **5** and washed; afterward they were incubated for 1 h with **1** and washed again. The results are reported in Figure 1C, showing the overlay of the corresponding fluorescence images taken 48 and 168 h (7 days) after treatment with the fluorophores. Immediately after uptake of both fluorophores, merging of green and red cellular labeling was visible. After 48 h, the cells were still proliferating and the fluorescence was transmitted from mother to daughter cells (see also Figure S29). A few days after treatment, a few green fluorescent fibrillar structures were detected while the red staining of cells cytoplasm by **5** became predominant. Apparently, the presence of the second fluorophore causes only some delay in the secretion of fluorescent fibrils.

Figure 2 shows that intensely green fluorescent fibrils were also produced by NIT 3T3 cells treated with DTTO fluorophores **2** and **3**. With **2** and **3** the formation of fibrils was slower than with **1**. Parts A-c and B-c of Figure 2 show fluorescent fibrils formed 72 h after treatment. Apparently, the size and morphology of the fibrils changed on changing the molecular structure of the fluorophore, shorter and in tight bundles with **2**, longer and more isolated with **3**.

Fluorophore **1** was also tested with HeLa cells, and also in this case the production of fluorescent fibrils was observed. The experiment carried out with HeLa cells is illustrated in Figure 2C.

The cells were incubated for 1 h with fluorophore **1** at different times, 18 and 72 h, after they had been seeded on Petri dishes. The cells were then washed to remove the unbound fluorophore,

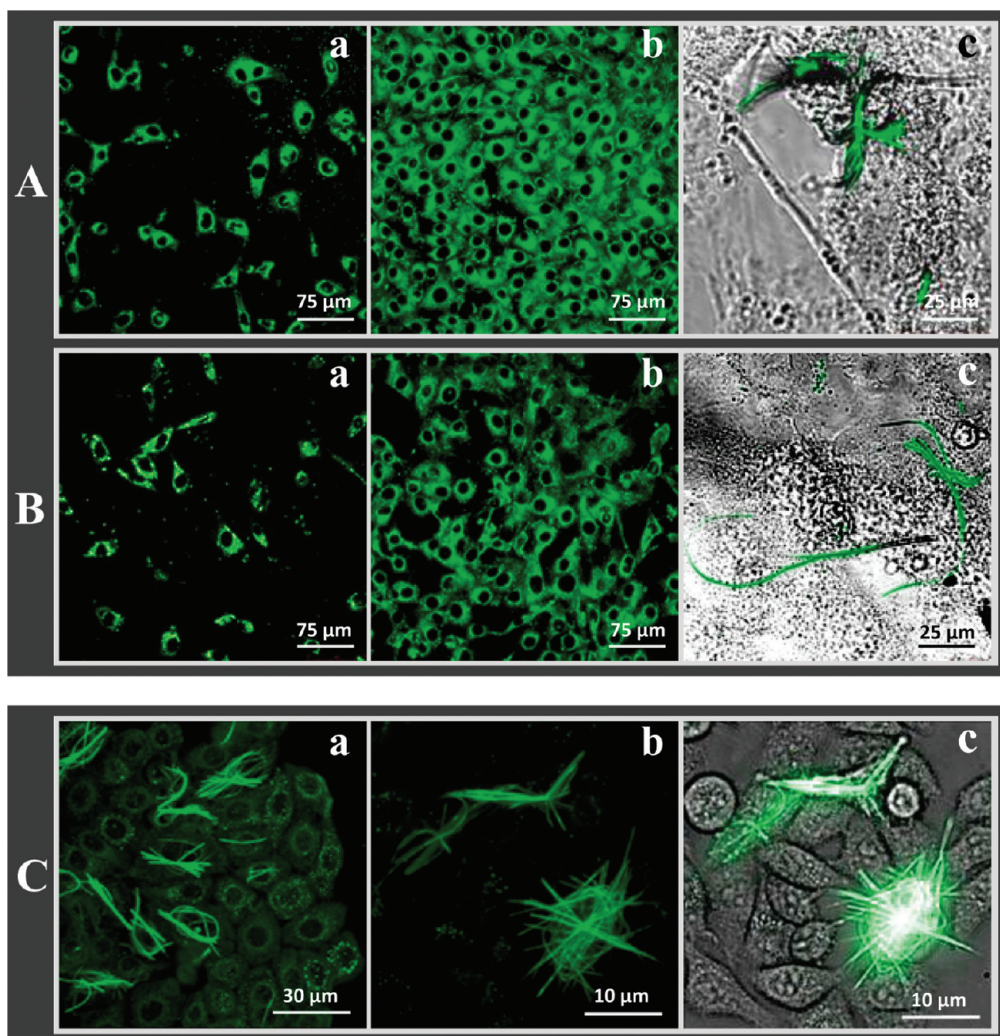


**Figure 2.** (A) LSCM images of NIH 3T3 cells stained with fluorophore 3 taken 1 h (a) and 48 h (b) after treatment and magnification of some fluorescent fibrils present 72 h after treatment (c, overlay of images from light transmission and fluorescence microscopies). (B) Same as A with fluorophore 2. (C) HeLa cells treated with fluorophore 1, 18 (a) and 72 h (b,c) after having been seeded on Petri dishes. Incubation with the fluorophore lasted for 1 h in both cases, and the images were taken 24 h after treatment.

and LSCM images were taken 24 h later in both cases. It was found that the amount of fibrils produced by cells treated 18 h after seeding was much higher than that produced by those treated 72 h after seeding. Interestingly, the latter cells showed the presence of green clusters around the perinuclear region, in particular in the rough endoplasmic reticulum, i.e., in the region of cells where proteins synthesis takes place (Figure 2Ca). This experiment suggested that the formation of fibrils was a physiological process and that the fibrils might have a proteic nature. We envisaged that the difference in the amount of fibrils produced could be due to the fact that the cells seeded 72 h before incubation with the fluorophore had already produced all the typical extracellular matrix proteins and remained in a stationary protein production phase, while those treated 18 h after seeding were still in a synthesis phase and were able to incorporate into the fibrils most of the fluorophore administered to the cells.

In agreement with the assumption that the formation of fluorescent fibrils was due to a cellular physiological process, repeated attempts to stain with DTTOs commercial fibrils of type-I collagen and other main extracellular matrix proteins, such

as laminin and fibronectin, invariably failed. No green fluorescent fibrils were obtained in these experiments, even using highly concentrated fluorophore solutions (see, for example, Figure S28).

The fluorophores were not toxic to the cells. This is illustrated in Figure 3, showing 3-(4,5-dimethylthiazol-2-yl)-2,5-diphenyltetrazolium bromide (MTT) cytotoxicity tests on NIH 3T3 cells treated with the different fluorophores compared to untreated cells. The tests indicate that all fluorophores but 4 were not toxic to the cells, their viability being near 80% or much more, even when the cells were secreting the fluorescent fibrils. Contrary to the treatment with the other fluorophores, treatment with 4 caused the viability of the cells to drop to less than 20%. This compound had a free terminal hydroxyl group, highly toxic to the cells. However, when the O–H functionality was protected with a MEM group ( $-\text{CH}_2\text{OCH}_2\text{CH}_2\text{OCH}_3$ ), as in 3, the fluorophore was no more toxic to the cells and contributed to the production of fluorescent fibrils.

**Fibrils Characterization.** Most of the fluorescent fibrils secreted by the cells in the presence of DTTO fluorophores displayed helical supramolecular organization. Some helical fluorescent fibrils formed by

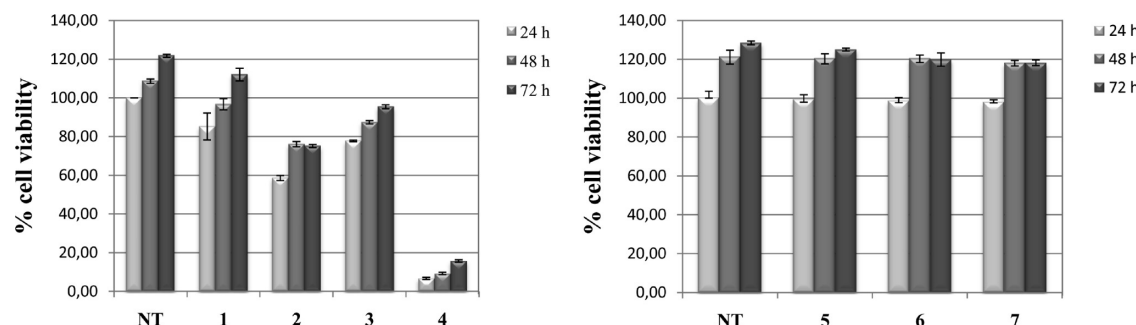


Figure 3. MTT cytotoxicity tests for NIH 3T3 cells treated with fluorophores 1–7 compared to untreated cells (NT).

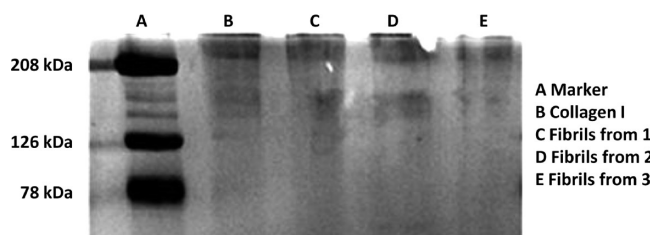


Figure 4. Sodium dodecyl sulfate–polyacrylamide gel electrophoresis of fluorescent fibrils formed by NIH 3T3 cells upon uptake of fluorophores 1–3 and isolation from the cells.

the cells and picked out by LSCM were isolated from cell medium and analyzed by sodium dodecyl sulfate–polyacrylamide gel electrophoresis (SDS-PAGE), the method commonly used to analyze proteins.

Figure 4 shows the SDS-PAGE carried out with fluorescent fibrils produced by NIH 3T3 fibroblasts 72 h after treatment with 1–3 and isolated from the cells (see SI for details). In this experiment the behavior of the fibrils was compared to that of commercial fibrils of type-I collagen, which is the predominant product of fibroblasts activity.<sup>26–28</sup> In Figure 4, lane A shows the bands of the molecular weight marker employed to monitor the progress of the electrophoretic run, lane B the bands of type-I collagen, and lanes C–E the bands pertaining to the fluorescent fibrils formed after treatment of the cells with 1–3. The irreversible staining with Coomassie Blue of the electrophoretically separated bands allowed the visualization of the separated proteins.

SDS-PAGE unambiguously indicated the proteic nature of the helical fluorescent fibrils, which were characterized by high molecular weights, similar to those of type-I collagen. Remarkably, the fibrils secreted by the cells upon treatment with 1–3 in separate experiments all displayed the same proteic composition.

Figure 5 shows LSCM images, spatially resolved photoluminescence spectra (SR-PL), and 3D LSCM images obtained by PL z-reconstruction of fibrils formed upon incubation of HeLa cells with fluorophore 1 and NIH 3T3 cells with fluorophore 3. For comparison, the supramolecular arrangement of the same fluorophores in cell culture medium (DMEM) but in the absence of cells is also reported. The figure shows that, in the absence of cells, the fluorophores form shapeless aggregates, emitting green light and characterized by a photoluminescence spectrum similar to that of the dyes in solution. By contrast, the fluorescent fibrils released in the presence of cells were well structured and characterized by fluorescence periodicity ranging from 2 to 10  $\mu\text{m}$ . The spatially resolved PL spectra along the fibrils structure showed an emission similar to that of the dyes in solution and a

modulation of the PL intensity related to the helical arrangement. In general, the fluorescence periodicity seemed to be related to the complexity of the superhelices (helices of helices) formed. A wide range of fibrils dimensions was always observed, probably depending not only on the molecular structure of fluorophore but also on the stage of development and the number of helices wrapped up in themselves.

The formation of helical superstructures was also observed by AFM topography. Figure 6A shows the AFM image of a fixed HeLa cell having adherent fluorescent fibrils (picked out by LSCM) obtained upon incubation with fluorophore 1. Figure 6B shows the AFM image of fluorescent fibrils obtained upon incubation of NIH 3T3 cells with fluorophore 2 and isolated from the cells. The helical structures in Figure 6 show the same structural periodicity measured by confocal microscopy with the helix step in the range of 2–5  $\mu\text{m}$ .

**Hypothesis for the Interaction of DTTO Fluorophores with Protocollagen Polypeptide Chains and Theoretical Calculations.** It is known that fibroblasts and other cell types in culture are able to produce collagen fibrils that are randomly distributed in the cell culture.<sup>26–29</sup> Collagen is the most abundant protein in mammals, synthesized predominantly in the form of type-I collagen and self-assembled into fibrillar triple helices.<sup>30</sup> The helical morphology of the fluorescent fibrils secreted by our cells in culture is in agreement with the fact that they contain collagen, as shown by electrophoretic analysis.

To account for our experimental results, we made the hypothesis that DTTO fluorophores are specifically recognized by some component of protocollagen polypeptide chains<sup>28–30</sup> and incorporated via nonbonding interactions at some stage during the self-assembly of protocollagen and the subsequent formation of collagen triple helices. The spontaneous aggregation of triple-helical collagen molecules into fibrils with embedded DTTOs renders the fibrils fluorescent and traceable by fluorescence techniques. The hypothesis appears reasonable in view of the fact that in vitro studies on collagen growth and self-assembly from synthetic collagen-mimetic peptides have demonstrated that the incorporation of exogenous compounds such as metal complexes can stabilize the triple helix of collagen,<sup>31</sup> probably via stereoelectronic effects.<sup>30,32,33</sup>

It is known that collagen consists of three left-handed helical chains coiled around each other to form a right-handed supercoil stabilized by interchain hydrogen bonds. The polypeptide chains of procollagen are made of approximately 300 repeats of the sequence Gly-X-Y, where Gly stands for glycine and X and Y are predominantly L-proline (Pro) and 4(R)-hydroxy-L-proline (HyPro).<sup>29</sup> For each Gly-X-Y triplet, there is a hydrogen bond

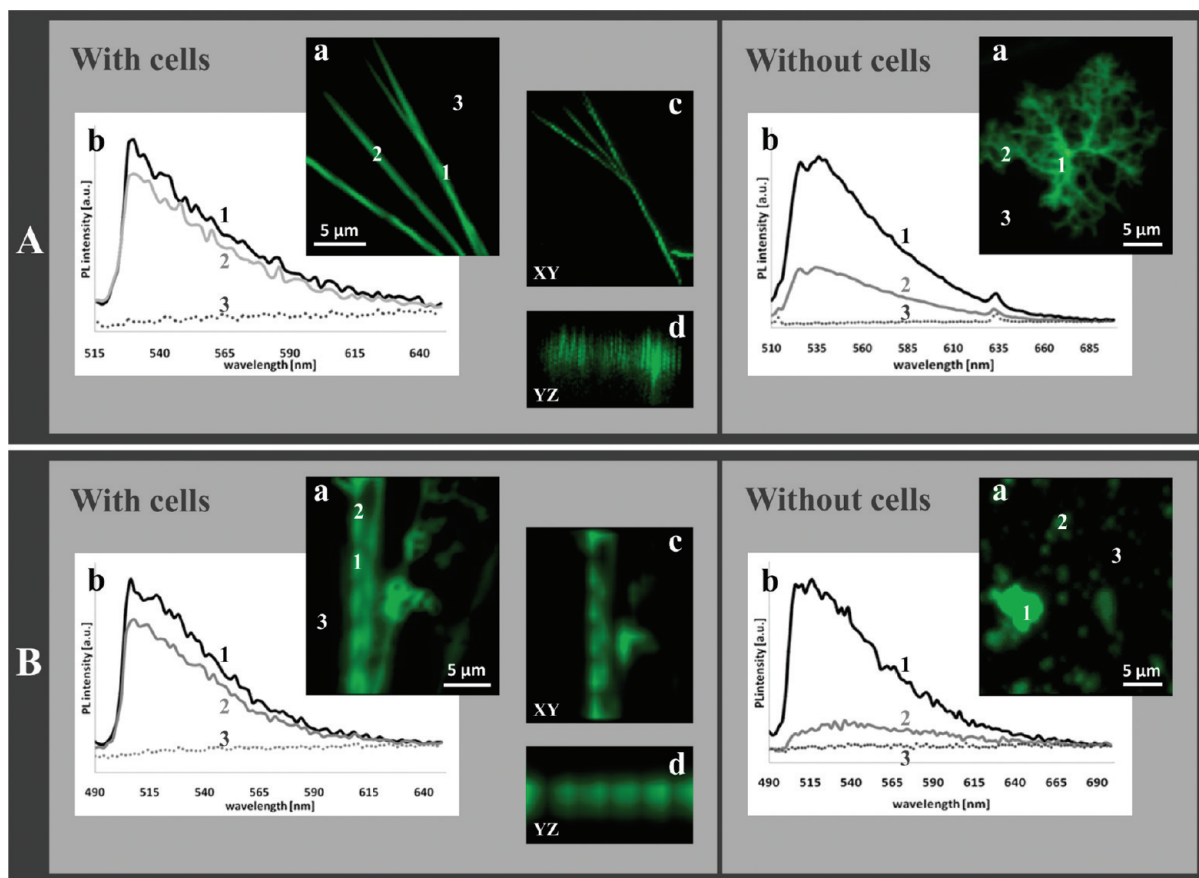


**Figure 5.** Laser scanning confocal microscopy (LSCM) images (a), spatially resolved photoluminescence spectra (SR-PL) (b), 3D LSCM images obtained by PL z-reconstruction (c), and the corresponding optical sections (d) of fibrils formed upon incubation of HeLa cells with fluorophore 1 (A) and upon incubation of NIH 3T3 cells with fluorophore 3 (B). For comparison, LSCM images (a) and spatially resolved photoluminescence spectra (SR-PL) (b) of self-assembled fluorophores 1 and 3 in the same medium used for cells culture (DMEM) but in the absence of cells are also reported.

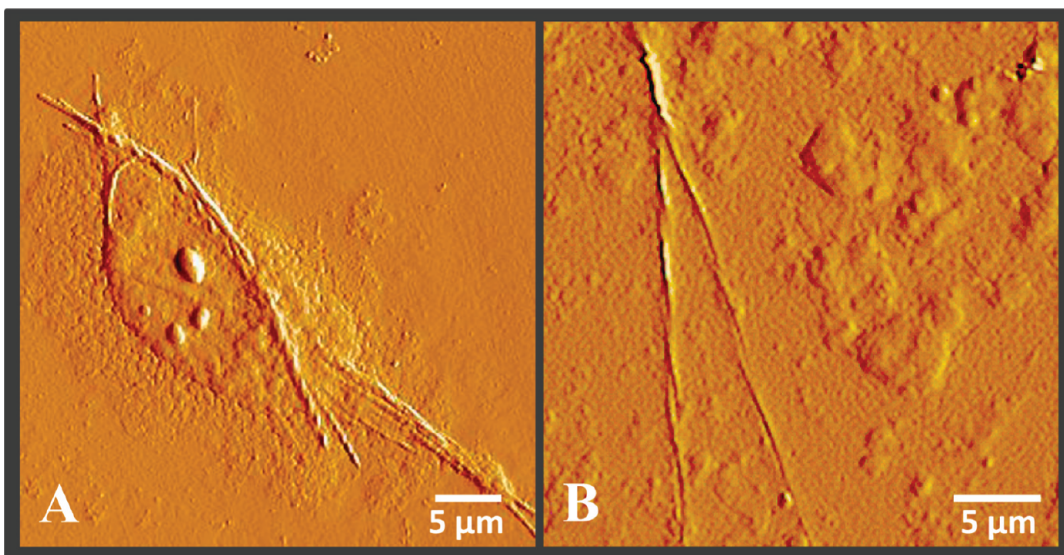


**Figure 6.** (A) AFM of a frozen HeLa cell treated with 1 and showing adherent helical fibrils. (B) AFM of helical fibrils formed by NIH 3T cells treated with 2 and isolated from the cells. LSCM showed that, in both cases, the helical fibrils were brightly green fluorescent.

between the amide hydrogen atom of Gly in one chain and the carbonyl oxygen atom of X in the adjacent chain.

We carried out theoretical calculations on a system consisting of three sequences of the tripeptide Gly-Pro-HyPro, as model for

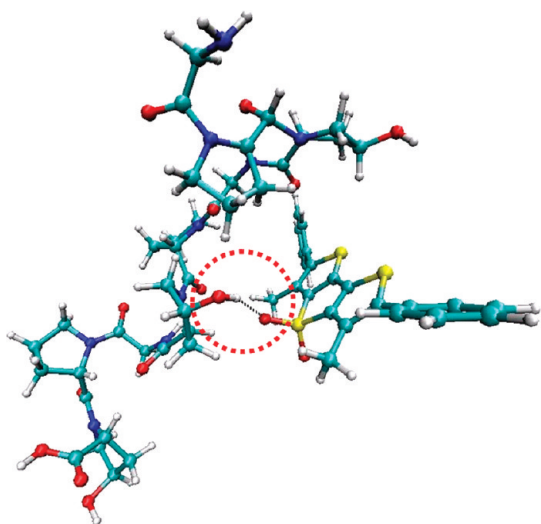


**Figure 7.** Calculated “complex” of fluorophore **1** with three sequences of the tripeptide Gly-Pro-HyPro (glycine-proline-hydroxyproline) as model for a collagen strand. The circle indicates the H-bonding formed in the inner tripeptide between the O—H group of HyPro and the O—S—O group of the dithienothiophene core of the fluorophore.

procollagen chains,<sup>32</sup> in the presence of fluorophore **1**, chosen since it is a symmetric molecule. The structure of isolated procollagen chain and **1** was preoptimized at the AM1 semi-empirical level.<sup>34</sup> A conformational search was then performed to probe the possible binding sites for **1** by performing 650 geometry optimizations at the AM1 level, starting from different relative positions of **1** and the polypeptide chain. The 10 optimized structures with the lowest energy were further optimized at the B3LYP/TZVP level<sup>35–38</sup> to refine the results and identify the binding site of **1** with the lowest total energy. The binding energy for the finally selected structure was computed at the B3LYP/TZVP level with a counterpoise procedure to correct for the basis set superposition error.<sup>38</sup> AM1 calculations were performed using GAUSSIAN03,<sup>39</sup> while B3LYP calculations were performed with the TURBOMOLE program package.<sup>40</sup> The results are shown in Figure 7. The calculations predicted an energetically favorable configuration (binding energy 8.2 kcal/mol, H-bond length 1.95 Å) involving a hydrogen bond between the HyPro and one of the oxygen atoms of **1**. According to the calculations, the plane of the inner DTTO core was parallel to the polypeptide axis, while the external phenyl rings were tilted by 58° and the oxygen atoms were on opposite sides of the plane, a geometry corresponding to that determined by X-ray analysis.<sup>22</sup>

The calculations support our hypothesis, according to which DTTO fluorophores are recognized by a component of collagen polypeptide chains—specifically HyPro—and incorporated via nonbonding interactions within the polypeptide chain. The periodicity of DTTO fixation through multiple hydrogen bondings, related to the presence of HyPro at regular distances into the procollagen polypeptide chains, creates periodicity in fluorescence emission at the nanometer scale. The fluorescence periodicity observed at the micrometer scale in the fibrils secreted by the cells is probably related to the wrapping up of several nanometer-sized fluorescent fibrils into themselves.

It is known that hydroxyproline coordinates a network of water molecules within the triple helix of collagen, forming intra-

or intermolecular bridges.<sup>30</sup> The inner core of DTTO fluorophores, with one oxygen above and one below the molecular plane, is in principle capable of forming bridges between proto-collagen chains, contributing to lateral fibrils growth during the self-assembly process. This matter will be the subject of further studies aimed at elucidating the precise supramolecular mechanism by which the fluorescent fibrils are built in the presence of DTTOs. In this respect, it is worth recalling that LSCM measurements (Figure 2) suggest that the molecular structure of the fluorophore might play a role in modulating the shape and dimension of the fluorescent fibrils and that it is known that incorporation of metal complexes<sup>31</sup> or the presence of macromolecules such as fibromodulin<sup>27,28</sup> can modulate the shape and the size of self-assembled collagen aggregates.

## CONCLUSIONS

We have described two classes of biocompatible thiophene fluorophores capable of spontaneously crossing the membrane of live cells: the first is capable of staining the cytoplasm through reaction of the N-succinimidyl ester functionality with primary amino groups of intracellular proteins; the second, based on the dithienothiophene-S,S-dioxide moiety (DTTO), is capable of participating in the physiological formation of fluorescent fibrils.

We have shown that live cells, upon spontaneous uptake of DTTO fluorophores, secrete collagen containing fluorescent fibrils, most of which display helical supramolecular organization. The process was tested repeatedly and the results were highly reproducible. Based on electrophoretic analysis, morphology and theoretical calculations, we interpreted these results on the basis of molecular recognition between the DTTO and the hydroxyproline component of procollagen polypeptide chains, leading to incorporation of the fluorophore through multiple hydrogen-bondings.

The results concerning DTTO fluorophores are the proof of principle that cell-permeant, small, and nontoxic fluorescent molecules can spontaneously transfer their properties to an intracellular protein in live cells through molecular recognition and participation in a supramolecular self-assembly process.

The spontaneous uptake of the DTTOs by live cells is not only a powerful strategy to visualize intracellular processes by fluorescence techniques but also an invaluable tool to introduce chemical diversity and additional properties into collagen forming within live cells, in a single step. As is the case with many conjugated molecules, besides fluorescence, DTTOs are also characterized by additional properties, in particular electroactivity.<sup>22</sup> Thus, DTTO fluorophores are potentially a vehicle to introduce electroactivity within collagen fibrils. Work is in progress in this direction with the objective of creating innovative classes of biocompatible and biologically active materials for biomedical applications.

## ASSOCIATED CONTENT

**S Supporting Information.** Full experimental details for the synthesis of **1–7** and their precursors; <sup>1</sup>H and <sup>13</sup>C NMR spectra of **1–7** and their precursors; UV-vis and PL spectra of **1–7**; fluorescence microscopy characterization of commercial synthetic ECM proteins treated with DTTO **1**; experimental details of cell staining; complete ref 39. This material is available free of charge via the Internet at <http://pubs.acs.org>.

**■ AUTHOR INFORMATION****Corresponding Author**

barbarella@isof.cnr.it

**■ ACKNOWLEDGMENT**

This research was supported by project FIRB RBPR05JH2P\_ITALNANONET and by ERC Starting Grant FP7 Project DEDOM (No. 207441).

**■ REFERENCES**

- (1) Hell, S. W. *Science* **2007**, *316*, 1153–1158.
- (2) Newman, R. H.; Fosbrink, M. D.; Zhang, J. *Chem. Rev.* **2011**, *111*, 3614–3666.
- (3) Krumova, K.; Cosa, J. *J. Am. Chem. Soc.* **2010**, *132*, 17560–17569.
- (4) Ueno, Y.; Jose, J.; Loudet, A.; Pérez-Bolívar, C.; Anzenbacher, P., Jr.; Burgess, K. *J. Am. Chem. Soc.* **2011**, *133*, 51–55.
- (5) Lu, Y.; Dasog, M.; Leontowich, A. F. G.; Scott, R. W. J.; Paige, M. F. *J. Phys. Chem. C* **2010**, *114*, 17446–17454.
- (6) Liu, W.; Howarth, M.; Greytak, A. B.; Zheng, Y.; G. Nocera, D.; Ting, A. Y.; Bawendi, M. G. *J. Am. Chem. Soc.* **2008**, *130*, 1274–1284.
- (7) Mahler, B.; Spinicelli, P.; Buil, S.; Quelin, X.; Hermier, J. P.; Dubertret, B. *Nat. Mater.* **2008**, *7*, 659–664.
- (8) Wu, C.; Schneider, T.; Zeigler, M.; Yu, J.; Schiro, P. G.; Burnham, D. R.; McNeill, J. D.; Chiu, D. T. *J. Am. Chem. Soc.* **2010**, *132*, 15410–15417.
- (9) Lee, H. D.; Lord, S. J.; Iwanaga, S.; Zhan, K.; Xie, H.; Williams, J. C.; Wang, H.; Bowman, G. R.; Goley, E. D.; Shapiro, L.; Twieg, R. J.; Rao, J.; Moerner, W. E. *J. Am. Chem. Soc.* **2010**, *132*, 15099–15101.
- (10) Kobayashi, H.; Choyke, P. L. *Acc. Chem. Res.* **2011**, *44*, 83–90.
- (11) Garner, L. E.; Park, J.; Dyar, S. M.; Chworus, A.; Sumner, J. J.; Bazan, G. C. *J. Am. Chem. Soc.* **2010**, *132*, 10042–10052.
- (12) Björka, P.; Nilsson, K. P. R.; Lenner, L.; Kagedal, B.; Persson, B.; Inganäs, O.; Jonasson, J. *Mol. Cell. Probe* **2007**, *21*, 329–337.
- (13) Li, K.; Pu, K. Y.; Cai, L.; Liu, B. *Chem. Mater.* **2011**, *23*, 2113–2119.
- (14) Resch-Ganger, U.; Grabolle, M.; Cavalieri-Jaricot, S.; Nitschke, R.; Nann, T. *Nat. Methods* **2008**, *5*, 763–775.
- (15) Goldys, E. M. *Fluorescence Applications in Biotechnology and Life Sciences*; Wiley-Blackwell: Hoboken, New Jersey, 2009.
- (16) *The Molecular Probes Handbook, A Guide to Fluorescent Probes and Labeling Technologies*, 11th ed.; Johnson, I., Spence, M. T. Z., Eds.; Life Technologies: Eugene, Oregon, 2010.
- (17) Zambianchi, M.; Di Maria, F.; Cazzato, A.; Gigli, G.; Piacenza, M.; Della Sala, F.; Barbarella, G. *J. Am. Chem. Soc.* **2009**, *131*, 10892–10900.
- (18) *Handbook of Thiophene-Based Materials*; Perepichka, I. E., Perepichka, D. F., Eds.; John Wiley & Sons: Chichester, 2009.
- (19) Duca, M.; Dozza, B.; Lucarelli, E.; Santi, S.; Di Giorgio, A.; Barbarella, G. *Chem. Commun.* **2010**, *46*, 7948–7950.
- (20) Suzuki, A. *Proc. Jpn. Acad., Ser. B* **2004**, *80*, 359–371.
- (21) Espinet, P.; Echavarren, A. M. *Angew. Chem., Int. Ed.* **2004**, *43*, 4704–4734.
- (22) Barbarella, G.; Favaretto, L.; Sotgiu, G.; Antolini, L.; Gigli, G.; Cingolani, R.; Bongini, A. *Chem. Mater.* **2001**, *13*, 4112–4122.
- (23) Becker, R. S.; Seixas de Melo, J.; Macanita, A. L.; Elisei, F. *J. Phys. Chem.* **1996**, *100*, 18683–18695.
- (24) Wang, X. Q.; Duan, X. M.; Liu, L. H.; Fang, Y. Q.; Tan, Y. *Acta Biochim. Biophys. Sin.* **2005**, *37*, 379–385.
- (25) Barbarella, G.; Zambianchi, M.; Ventola, A.; Fabiano, E.; Della Sala, F.; Gigli, G.; Anni, M.; Bolognesi, A.; Polito, L.; Naldi, M.; Capobianco, M. *Bioconjugate Chem.* **2006**, *17*, 58–67.
- (26) Falini, G.; Fermani, S.; Foresti, E.; Parma, B.; Rubini, K.; Sidoti, M. C.; Roveri, N. *J. Mater. Chem.* **2004**, *14*, 2297–2302.
- (27) Canty, E. G.; Kadler, K. E. *J. Cell Sci.* **2005**, *118*, 1341–1353.
- (28) Hulmes, D. J. S. *J. Struct. Biol.* **2002**, *137*, 2–10.
- (29) Prockop, D. J.; Fertala, A. *J. Biol. Chem.* **1998**, *273*, 15598–15604.
- (30) Shoulders, M. D.; Raines, R. T. *Annu. Rev. Biochem.* **2009**, *78*, 929–958.
- (31) Marcos, M. P.; Chmielewski, J. *J. Am. Chem. Soc.* **2009**, *131*, 2706–2712.
- (32) Improta, R.; Mele, F.; Crescenzi, O.; Benzi, C.; Barone, V. *J. Am. Chem. Soc.* **2002**, *124*, 7857–7865.
- (33) Hodges, M. D.; Raines, R. T. *J. Am. Chem. Soc.* **2005**, *127*, 15923–15932.
- (34) Dewar, M. J. S.; Zoebisch, E. G.; Healy, E. F.; Stewart, J. J. P. *J. Am. Chem. Soc.* **1985**, *107*, 3902–3909.
- (35) Becke, A. D. *J. Chem. Phys.* **1993**, *98*, 5648–5652.
- (36) Lee, C.; Yang, W.; Parr, R. G. *Phys. Rev. B* **1988**, *37*, 785–789.
- (37) Schäfer, A.; Huber, C.; Ahlrichs, R. *J. Chem. Phys.* **1994**, *100*, 5829–5835.
- (38) van Duijneveldt, F. B.; van Duijneveldt-van de Rijdt, J. G. C. M.; van Lenthe, J. H. *Chem. Rev.* **1994**, *94*, 1873–1885.
- (39) Frisch, M. J.; et al. *Gaussian 03*, Revision C.02; Gaussian, Inc.: Wallingford, CT, 2004.
- (40) Ahlrichs, R.; Bär, M.; Häser, M.; Horn, H.; Kölmel, C. *Chem. Phys. Lett.* **1989**, *162*, 165–169.
- (41) Geng, Y.; Li, H.; Wu, S.; Duan, Y.; Su, Z.; Liao, Y. *Theor. Chem. Acc.* **2011**, *129*, 247–255.